

Active control of thermal emission by graphene-nanowire coupled plasmonic metasurfaces

Jiayu Li, Zhuo Li, Xiu Liu, and Sheng Shen*

Department of Mechanical Engineering, Carnegie Mellon University, Pittsburgh, Pennsylvania 15213, USA

Stanislav Maslovski

*Department of Electronics, Telecommunications and Informatics,
University of Aveiro, Campus Universitário de Santiago, 3810-193 Aveiro, Portugal*

(Dated: March 23, 2022)

Metasurfaces, together with graphene plasmonics, have become prominent for the emissivity control in thermal engineering, both passively through changing the geometric parameters and packing density of the metasurfaces, and actively through graphene gating or doping. We demonstrate a graphene-nanowire coupled plasmonic metasurface utilizing the hybrid localized surface plasmon modes of the nanowire array and graphene. The nanowire array makes the hybrid surface plasmon mode localized, allowing a free-space excitation. The single layer graphene, via the gating between the underneath mirror and a top electrode, can actively tune the spectral emissivity by almost 90%. In addition, the hybrid plasmon mode provides an extra degree of freedom to modulate the p-polarized emissivity with a five-fold enhancement, especially for large emission angles.

I. INTRODUCTION

Thermal radiation, which physically originates from the spontaneous emission of thermally induced random currents in materials, is fundamental in many modern applications, including biological and chemical sensing¹, thermal imaging and camouflage^{2,3}, energy conversion and harvesting^{4,5}, and radiative cooling⁶. Compared to the isotropic and incoherent thermal emission from bulk surfaces, nanostructure-based metasurfaces have been successfully applied to precisely control the emissivity both spectrally⁷ and spatially⁸. Based on the Purcell effect, the sub-wavelength nanostructure, which supports localized surface plasmon polaritons, can serve as an optical resonator to drastically modulate the response of the nanostructure at designed resonant frequencies. The coupling between these ‘meta-atoms’, which is well described by a tight bonding model⁹ or coupled mode theory¹⁰, provides rich degrees of freedom for the design of the metasurface.

Recently, graphene plasmonics has attracted extensive attention to further boost the plasmonic effects in thermal radiation engineering¹¹⁻¹⁴. Graphene, a two-dimensional single layer of carbon atoms, can support surface plasmon polaritons with a stronger optical confinement as compared to conventional noble metals. It has been reported that graphene nanostructures enable to manipulate the light in a dimension on the order of 10^{-2} times smaller than the free-space wavelength¹¹. This excellent beyond-diffraction-limit performance plays a critical role in bridging the nanoscale electronic devices and microscale photonic devices. In addition, the graphene plasmons excited in the mid-infrared range typically exhibit low loss, resulting in a stronger spectral coherence for thermal radiation¹⁵. More importantly, the optical responses of graphene can be actively tuned by changing its charge carrier density via gating

or doping^{16,17}. Together with the improving maturity of graphene transfer and patterning, graphene plasmonic metasurfaces become a promising complement to traditional metal plasmonics and pave the way for the ultra-fast control of thermal radiation.

In this paper, we propose a graphene-nanowire coupled metasurface working at mid-infrared wavelengths, as shown in Figs. 1 (a) and (b). The nanowire array makes the hybrid surface plasmon mode localized, allowing a free-space excitation. The single layer graphene, via the gating between the underneath mirror and a top electrode, can actively tune the thermal emission spectrally and spatially.

II. GRAPHENE AND NANOWIRE ARRAY COUPLED SYSTEM

To demonstrate the physics associated with the graphene-nanowire hybrid surface plasmon mode, we start from a single gold nanowire with a length of $2.5 \mu\text{m}$ and a cross-section area of 150 nm (x -direction) by 180 nm (y -direction) directly on top of an intrinsic single graphene layer. A 30 nm thick layer of HfO_2 is under the graphene acting as the dielectric spacer for electrical gating. Another 70 nm thick gold layer under the HfO_2 serves as an optical mirror as well as the electrical gating electrode, as shown in Fig. 1 (b).

The gold nanowire can support multiple resonant plasmonic modes at different wavelengths. Our finite-difference time-domain (FDTD) simulation together with the Wiener chaos expansion method^{18,19} shows the first direct emission resonant mode which manifests a typical dipole-like resonance characteristic with charges accumulated at the two ends of the nanowire, as shown in Fig. 2 (a).

Without gating, only the localized surface plasmon modes from the gold nanowire can be observed, since the

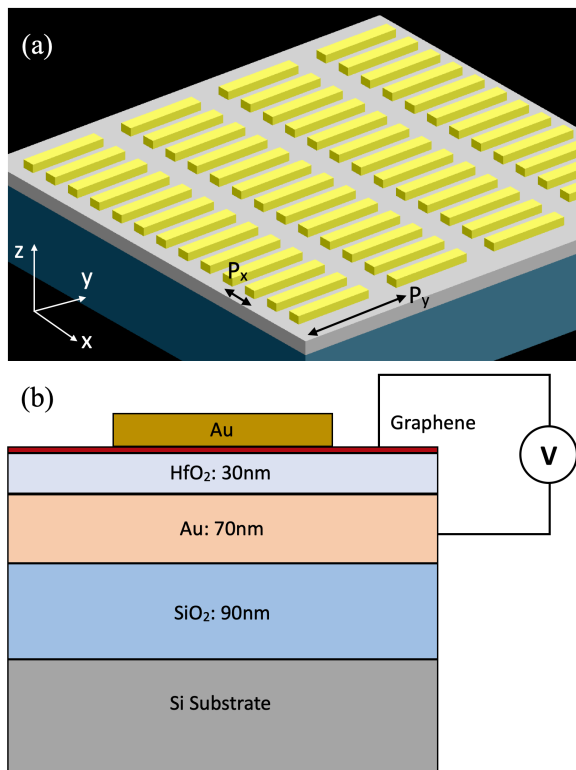


FIG. 1. (a) Schematic of graphene-nanowire coupled metasurface. P_x and P_y represent the periodicity of the nanowire array in the x - and y -directions, respectively. (b) Cross-section of the graphene-nanowire coupled metasurface. Electrical gating of graphene is achieved via the underneath Au mirror and the top electrode.

intrinsic graphene performs like a dielectric layer. By gating the graphene layer, it behaves like a metallic material due to the extra free electrons, and thus surface plasmon modes can be excited at the metal-dielectric interface. The single nanowire then functions as the near-field scattering tip to efficiently excite the surface plasmon modes along the graphene layer. As we excite the graphene-nanowire system, not only the nanowire resonant modes but also the graphene surface plasmon can be excited, as shown in Fig. 2 (b). When the single nanowire deposited on the graphene layer functions as the scattering tip, the surface plasmon modes supported by the graphene layer will continuously extend to the entire graphene layer until their energy completely decays. Such hybrid surface plasmon modes formed by the localized resonant modes inside the nanowire and the propagating modes supported inside the graphene are the key to actively modulate the optical properties of the metasurface. The modulation speed can be much faster than that induced by the thermo-optical effect. Once the nanowire array is introduced and forms a metasurface above the graphene layer, the continuous surface plasmon modes supported by the graphene will then be transformed into the localized ones. As one can see from Fig. 2 (c), the graphene

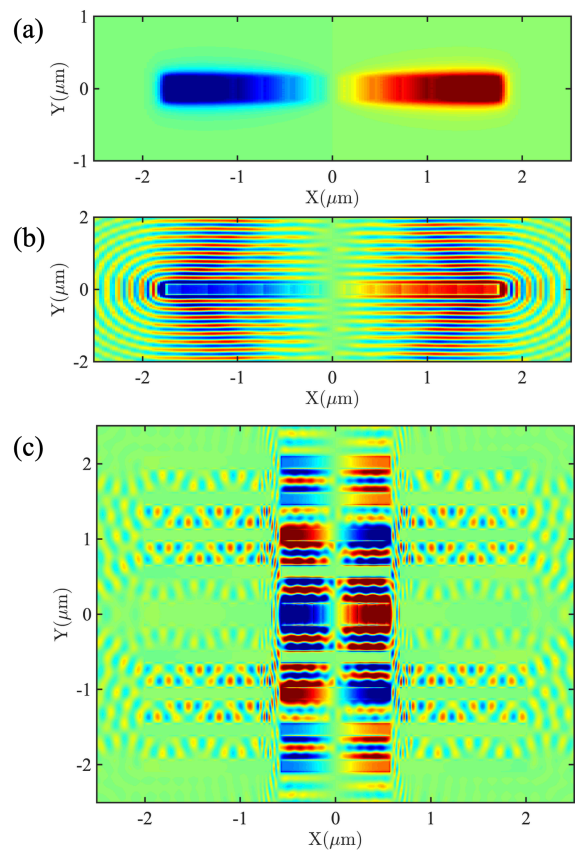


FIG. 2. (a) Fundamental resonant mode excited within the single nanowire on the intrinsic graphene layer. (b) Hybridized surface plasmon mode excited within the single nanowire on the gated graphene layer with the Fermi level at 0.4 eV. (c) Hybridized surface plasmon mode excited within the nanowire array on the gated graphene layer with Fermi level at 0.4 eV.

surface plasmon modes are excited and trapped by the contact points between the nanowires and graphene layer. The emissivity of such metasurface can be controlled by either changing the packing density of the nanowires passively or gating the graphene layer actively.

To make the graphene-nanowire hybrid metasurface working (near-perfectly absorptive) at mid-infrared wavelengths, we extend the gold nanowires with periodicities of $P_x = 0.5 \mu\text{m}$ and $P_y = 3 \mu\text{m}$, as shown in Fig. 1 (a). The emissivity of the system is calculated by simulating its absorptivity to the incoming linearly polarized plane wave, based on Kirchhoff's law. The electric field of the plane wave is parallel with the principal axis of the nanowire. The corresponding metasurface emissivity can then be found to dramatically change from 0.05 to 0.8 at the wavelength about $10.5 \mu\text{m}$ when the Fermi level of the graphene is tuned from 0.4 eV to 0.1 eV, as shown in Fig. 3 (a).

Such control of the emissivity at a certain wavelength is achieved based on the shifting and splitting of the nanowire resonant modes. As shown in Fig. 2 (c), the

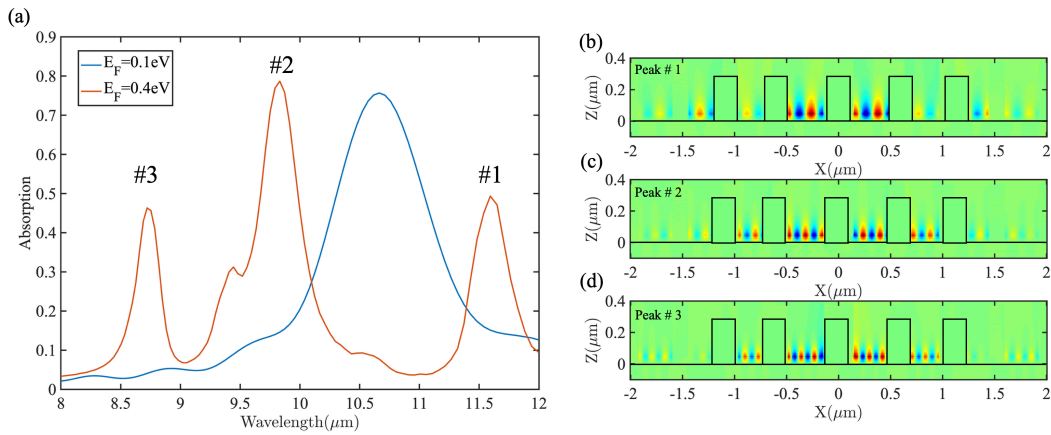


FIG. 3. (a) The modulation of the absorption (emission) spectrum for the graphene-nanowire metasurface. Nearly 90% of the change in the absorption spectrum around $10.5 \mu\text{m}$ in wavelength is observed when the Fermi level of graphene is changed from 0.1 eV to 0.4 eV due to the mode splitting. (b)–(d) Electric field profiles corresponding to peaks #1 to #3, respectively.

hybrid plasmonic mode is formed by two main contributions: the intrinsic resonant modes of the gold nanowires themselves; and the localized surface plasmon modes existing inside the cavity created by the adjacent nanowires and the graphene layer. When the graphene layer is not gated, no surface plasmon mode is supported, and the original resonant peak of the gold nanowire is preserved at $10.5 \mu\text{m}$. When the graphene layer is electrically gated, it becomes metallic and starts to support the surface plasmon modes. The first resonant mode of the gold nanowire hybridizes with the graphene surface plasmon modes of different orders and splits into multiple peaks around the original peak wavelength. In Fig. 3 (a), we plot the emission spectrum of the graphene and gold nanowire array at two graphene Fermi levels. When the Fermi level is 0.1 eV , the carrier density in graphene is relatively low and hence surface plasmon modes are not supported in graphene. The original nanowire resonant mode peak is still preserved at $10.5 \mu\text{m}$. As we increase the Fermi level up to 0.4 eV , the major resonant peak at $10.5 \mu\text{m}$ splits into three peaks at $8.7 \mu\text{m}$, $9.7 \mu\text{m}$, and $11.7 \mu\text{m}$ due to hybridization of the plasmon modes in the gold nanowire and in graphene. The corresponding electric field profiles (x - z plane) of these three peaks are plotted in Figs. 3 (b)–(d). Different spatial periodicities of the electric field are observed in the three cases and label the order of the modes, among which peak #1 is the surface plasmon mode of the lowest order, and peak #3 is the highest order mode in the wavelength range of interest. The number of the hybridized peaks around the original nanowire resonant modes and the spectral distance between them can be controlled by the gap distance between the adjacent nanowires. In general, the smaller the gap distance between adjacent nanowires, the smaller the number of the hybridized modes is and the larger the spectrum distance between them is. Ideally, carefully designing the pattern periodicity and the gold nanowire parameters can shift the desired wavelength to

a target value in the mid-infrared spectrum.

III. P-POLARIZATION ENHANCEMENT OF THE GRAPHENE-NANOWIRE ARRAY SYSTEM

Due to the highly polarized dipole-like radiation mode of the single nanowire, the nanowire metasurface usually exhibits a low emissivity when excited by the p-polarized electromagnetic wave (i.e., the E-field polarization is perpendicular to the principal axis of the nanowires, as shown in Fig. 4 (a)). Here we demonstrate that such p-polarized emissivity can be significantly enhanced for the graphene-nanowire array system when graphene is gated, especially for large incident angles, as indicated by α in Fig. 4 (a).

Figure 4 (b) plots the emissivity of the metasurface when the Fermi level of graphene is set to 0 eV . In this case, the incoming plane wave source cannot efficiently excite the metasurface due to the polarization mismatch, which results in the relatively low emissivity. Despite the overall low value, a peak centered around $8.5 \mu\text{m}$ can be noticed for the cases where $\alpha = 33.3^\circ$ and $\alpha = 40.0^\circ$, and another centered around $11 \mu\text{m}$ can be noticed for $\alpha = 40.0^\circ$, which correspond to the surface plasmon modes of the graphene excited by the scattered light from nanowires and can be utilized to enhance the p-polarized emissivity of the system.

To achieve this, we electronically gate the graphene layer so that its Fermi level reaches 0.6 eV . The simulated spectral emissivities are plotted in Fig. 4 (c). A narrow peak centered at the wavelength of $11.3 \mu\text{m}$ is observed for the incident angle α of the light between 20.0° to 40° . Specifically, compared to the ungated cases shown in Fig. 4 (b), a five-fold increase in the emissivity at the wavelength of $11.3 \mu\text{m}$ is observed for the cases where the incident angle α is between 26.67° to 40° .

Such enhancement of the p-polarized emissivity is at-

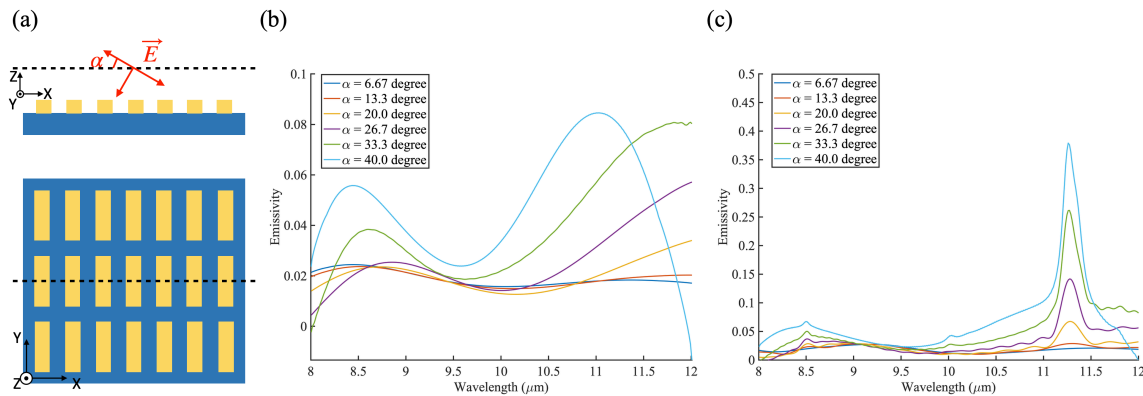


FIG. 4. Angular dependence of the emissivity for the graphene nanowire array system when the incident electric field is perpendicular to the principal axis of the golden nanowire. (a) Schematic of the oblique incidence of the light onto the metasurface at angle α when the periodicity of the nanowire array is $0.3 \mu\text{m}$ in the x -direction and $3 \mu\text{m}$ in the y -direction. The angular dependent spectral emissivity of the metasurface when the graphene Fermi level is tuned to be 0 eV [panel (b)] and 0.6 eV [panel (c)].

tributed to the coupling between the nanowire resonant modes and the graphene surface plasmon modes. Even though the p-polarized wave cannot effectively excite the resonant modes of the nanowire array, the scattered light from the nanowires will be able to excite the surface plasmon modes inside the graphene layer, especially for the large incident angle α . The surface plasmon modes of the graphene may then serve as a secondary source to excite the dipole-mode of nanowires, which produces the sharp peak near the intrinsic resonance frequency of nanowires. As a result, the hybridized plasmonic modes are invoked and contribute to the enhanced absorptivity of the p-polarized light, and by Kirchhoff's law, the thermal emissivity of the coupled metasurface. Such enhancement relieves the strict dependence on the polarization of the incident light. Furthermore, the Fermi level of graphene, together with the incident angle α , provides extra degrees of freedom for the thermal radiation manipulation of the graphene-nanowire array system.

IV. CONCLUSION

We develop a graphene-nanowire coupled metasurface utilizing the hybrid localized surface plasmon modes of the nanowire array and graphene. Thermal excitation can excite both the resonant modes of the nanowire array and the graphene surface plasmon modes trapped at the contact points between the nanowire and the graphene

layer. These coupling modes can drastically tune the emissivity of the metasurface passively through changing the geometric parameters and packing density of the nanowire array, and more importantly, actively through graphene gating. The peak positions and corresponding magnitudes of spectral emissivity can be modulated into target values through controlling the graphene Fermi level via electrical gating. In addition, because of the excitation of graphene localized surface plasmon modes, the p-polarized emissivity of the metasurface can be enhanced, especially for large emission angles. To conclude, the graphene-coupled nanowire metasurface is a promising platform for dynamic control of mid-infrared thermal radiation.

The data that support the findings of this study are available from the corresponding authors upon request²⁰.

ACKNOWLEDGMENTS

This work was primarily supported by the Defense Threat Reduction Agency (Grant No. HDTRA1-19-1-0028). This work was also funded partially by the National Science Foundation (Grant No. CBET-1931964). S. S. and S. M. acknowledge funding from Fundação para a Ciência e a Tecnologia (FCT), Portugal, under the Carnegie Mellon Portugal Program (project ref. CMU/TIC/0080/2019).

The authors declare no competing financial interest.

* sshen1@cmu.edu

¹ A. Lochbaum, Y. Fedoryshyn, A. Dorodnyy, U. Koch, C. Hafner, and J. Leuthold, *ACS Photonics* **4**, 1371 (2017).

² Y. Li, X. Bai, T. Yang, H. Luo, and C.-W. Qiu, *Nature Communications* **9**, 273 (2018).

³ O. Salihoglu, H. B. Uzlu, O. Yakar, S. Aas, O. Balci, N. Kakenov, S. Balci, S. Olcum, S. Süzer, and C. Kocabas, *Nano Letters* **18**, 4541 (2018).

⁴ D. M. Bierman, A. Lenert, W. R. Chan, B. Bhatia, I. Celanović, M. Soljačić, and E. N. Wang, *Nature En-*

- ergy **1**, 1 (2016).
- ⁵ D. Fan, T. Burger, S. McSherry, B. Lee, A. Lenert, and S. R. Forrest, *Nature* **586**, 237 (2020).
 - ⁶ A. P. Raman, M. A. Anoma, L. Zhu, E. Rephaeli, and S. Fan, *Nature* **515**, 540 (2014).
 - ⁷ B. Liu, J. Li, and S. Shen, *ACS Photonics* **4**, 1552 (2017).
 - ⁸ B. Yu, J. Li, and S. Shen, *Journal of Photonics for Energy* **9**, 032712 (2019).
 - ⁹ J. Li, B. Yu, and S. Shen, *Physical Review Letters* **124**, 137401 (2020).
 - ¹⁰ L. Zhu, S. Sandhu, C. Otey, S. Fan, M. B. Sinclair, and T. Shan Luk, *Applied Physics Letters* **102**, 103104 (2013).
 - ¹¹ F. H. L. Koppens, D. E. Chang, and F. J. García de Abajo, *Nano Letters* **11**, 3370 (2011).
 - ¹² H. Yan, T. Low, W. Zhu, Y. Wu, M. Freitag, X. Li, F. Guinea, P. Avouris, and F. Xia, *Nature Photonics* **7**, 394 (2013).
 - ¹³ V. W. Brar, M. C. Sherrott, M. S. Jang, S. Kim, L. Kim, M. Choi, L. A. Sweatlock, and H. A. Atwater, *Nature Communications* **6**, 7032 (2015).
 - ¹⁴ Q. Guo, C. Li, B. Deng, S. Yuan, F. Guinea, and F. Xia, *ACS Photonics* **4**, 2989 (2017).
 - ¹⁵ M. Jablan, H. Buljan, and M. Soljacic, *Physical Review B* **80**, 245435 (2009).
 - ¹⁶ C.-F. Chen, C.-H. Park, B. W. Boudouris, J. Horng, B. Geng, C. Girit, A. Zettl, M. F. Crommie, R. A. Segalman, S. G. Louie, and F. Wang, *Nature* **471**, 617 (2011).
 - ¹⁷ D. K. Efetov and P. Kim, *Physical Review Letters* **105**, 256805 (2010).
 - ¹⁸ J. Li, B. Liu, and S. Shen, *Physical Review B* **96**, 075413 (2017).
 - ¹⁹ Z. Li, J. Li, X. Liu, H. Salihoglu, and S. Shen, *Physical Review B* **104**, 195426 (2021).
 - ²⁰ The data that support the findings of this study are available from the corresponding authors upon request.